Time-resolved measurements of emission and absorption in a long pulse duration XeCl* laser

D.C. Hogan, A.J. Kearsley, C.E. Webb, R. Bruzzese

J. Physique **45** (1984) 1449-1456 SEPTEMBRE **1984,** PAGE 1449

Classification
Physics Abstracts
52.80 — 42.55

Time-resolved measurements of emission and absorption in a long pulse duration XeCl* laser (+)

D. C. Hogan, A. J. Kearsley, C. E. Webb and R. Bruzzese (*)

The Clarendon Laboratory, Parks Road, OX1 3PU Oxford, U.K.
(*) Istituto di Fisica Sperimentale dell'Università di Napoli, Pad. 20 Mostra d'Oltremare, 80125 Napoli, and Gruppo Nazionale Elettronica Quantistica e Plasmi del C.N.R., Italy

(*Reçu le 28 décembre 1983, révisé le 18 avril 1984, accepté le 10 mai 1984*)

Résumé. — Cet article décrit des études d'absorption et d'émission menées avec résolution temporelle sur une décharge laser XeCl*. Ce travail a été conduit pour mieux comprendre les mécanismes provoquant un arrêt prématuré des émissions spontanées ou laser. Ce phénomène est caractéristique de tout laser à halogénure de gaz rares excité par décharge. Nos résultats démontrent sans ambiguïté que la cause première de l'arrêt d'émission laser est la constriction du volume de la décharge. En outre il est montré que la présence de HCl dans le mélange est à l'origine de ce phénomène de constriction.

Abstract. — In this paper we describe time-resolved absorption and emission studies of an XeCl* laser discharge. The studies we carried out in order to gain a better understanding of the causes leading to the premature termination of both spontaneous emission and laser pulses in our device. This is a feature showed by all discharge pumped rare gas halide lasers.

1. Introduction.

We have previously reported [1, 2] investigations of the response of a resistively-ballasted discharge XeCl* laser to a relatively long (500 ns) excitation pulse applied at very low pulse repetition frequency (1 pps). Except for e-beam pumped devices, the laser pulse obtained under those conditions has the longest duration (270 ns FWHM, 20 kW peak power) yet reported for any XeCl* laser. The striking feature of these results was that, although the power input to the discharge volume was fairly constant (750 kW/cm^3) for a full 500 ns, the intensity of spontaneous emission showed a dramatic premature fall approximately 150 ns before the end of the discharge excitation pulse. The laser output showed similar premature termination. Other rare gas halide (RGH) lasers (as KrF*, ArF*, etc.) suffer from very similar limitations.

More generally, the laser output premature termination shows to be a problem in different kinds of electrically excited RGH laser devices. For example, Tailor [3] has recently performed a framing camera study of the temporal evolution of discharge uniformity in an X-ray preionized XeCl* laser with a reasonably long (150 ns) discharge excitation pulse. He has found that termination of laser output from his device is closely associated with the appearance of many filamentary channels in the discharge. Other authors [4, 5], who carried out much work on X-ray preionized XeCl* systems, found the same kind of problems associated with premature termination of laser output.

For these reasons, we carried out time-resolved measurements of emission and absorption in our laser discharge as a further means of characterizing the behaviour of the device, and of getting a deeper insight into the cause of the laser output premature termination.

In particular, three distinct experiments are described in this paper :

a) measurements of time-resolved absorption of ultraviolet radiation at selected wavelengths (i.e. those readily available) by our laser discharge : short duration (~ 20 ns) laser pulses (193, 243, 337 and 353 nm) were passed through the laser discharge at different times during the 500 ns discharge pulse (section 2);

(+) Please, contact Riccardo Bruzzese for reprints requirements.

b) measurements of time-resolved emission from the laser discharge from 300 nm to 600 nm, concentrating particularly on xenon neutral and ion emission lines (section 3);

c) measurements of time-resolved absorption in visible range by the laser discharge : the short duration (~ 20 ns), high-intensity, broad spectral band (460-490 nm) fluorescence pulse from a laser pumped dye was passed through the laser discharge of our device at different times during the discharge pulse (section 4).

The indications and the conclusions drawn from these experiments are discussed in section 5, where they are also related to our previous results which showed the discharge to constrict into a number of filamentary channels after 250 ns (see Refs. [1] and [2]). At this point, we would like to stress that many results obtained analysing the behaviour of our specific laser device, are more generally applicable to the problem of discharge stability in high pressure, strongly electron-attaching gas mixtures [6-9].

A full description of the laser device used throughout the experiments can be found in reference [1]. We just remember that : a charging voltage of 35 kV, discharged into the laser *via* a triggered spark gap, was used; the gas mixture normally used was 0.1 % HCl : 1.1 % Xe : 98.8 % Ne (or He), at 2.33 atmospheres overall; the UV preionization was supplied by a linear array of arcs.

2. Transient absorptions in the ultraviolet.

The experimental arrangement which was used for measuring transient absorptions in the UV is set out in figure 1. A rare gas halide (RGH) laser (« Oxford Lasers KX10 ») provided short duration (~ 20 ns) laser pulses at various UV wavelengths (353 nm, XeF*, 337 nm, N_2; 249 nm, KrF*; 193 nm, ArF*) depending on the gas mixture with which it was filled.

This light was used to probe our laser discharge for absorption at different times during the 500 ns excitation pulse of our device. Low jitter (~ 5 ns) triggering of the laser discharge and the probe laser was achieved by employing a « master » spark gap to provide fast-rising HV trigger pulses, *via* delay cables of adjustable length, to the main spark gap of each device.

Pairs of slits were placed at each end of the absorption cell (our laser): each pair consisted of two similar (1.5 mm × 2 cm) slits separated by 1.5 cm. The top slit at each end defined a path through the discharge region of the absorption cell for the probe radiation; the lower slit at each end defined a path through a similar length of laser gas outside the discharge for a reference beam. The reference beam was used to reduce problems associated with the shot-to-shot reproducibility of the KX 10 laser and the build-up of passive absorbing species within the absorption cell over the duration of a « run ».

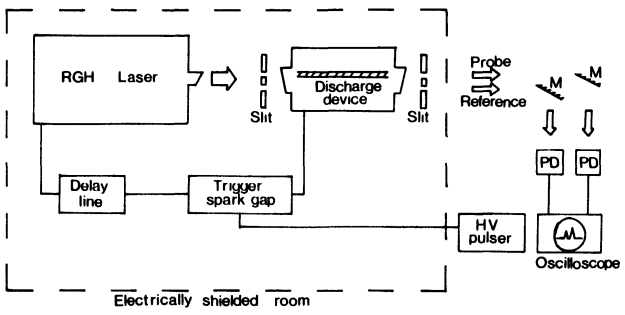

Fig. 1. — Experimental set-up for UV transient absorption measurements (see text for a full description). M = mirror; PD = photodiode.

The separate probe and reference beams emerging from the far end of the absorption cell were passed through a porthole in the Faraday cage laboratory and onto two fast UV sensitive photodiodes (one for each beam). The pulses were directed into a fast storage oscilloscope and their peak heights were measured. A 100 ns coaxial-cable delay line was introduced between the photodiode, which detected the probe pulse and the oscilloscope to separate the two signals. It was confirmed that this cable delay did not alter the measured peak height of the probe pulse.

In the case of transient absorption of ArF* radiation, each data point was arrived at by taking the mean of ten shots; the mean of five shots was obtained at all other wavelengths. The peak height of the probe signal was divided by the peak height of the reference signal for each shot taken.

A clear view of the functional dependence of the UV transient absorption with wavelength for a helium buffered laser mixture — HCl (2 mbar) + Xe (25 mbar) + He (2.3 Atm) — can be obtained by examination of figure 2. Absorption in neon buffered discharges showed a similar trend. It must be noted that absorption at times greater than 500 ns (i.e. after the initial

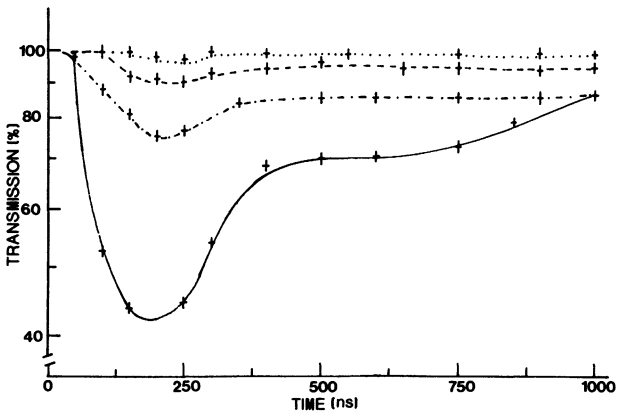

Fig. 2. — Transient absorption in the laser discharge at 353 nm (. . . .), 337 nm (------), 249 nm (—. —.), and 193 nm (——).

discharge pulse) was due to the fact that power continued to be delivered to the discharge at these late times as a consequence of voltage and current « ringing » in the circuit.

Two main features can be singled out : a) a decrease in the absorption, at any time, when increasing the laser probe wavelength; b) a dramatic absorption decrease, at any wavelength, after about 250 ns from discharge onset.

As well known, transient loss is possibly the single largest unknown which affects laser performance. The correct interpretation of experimental measurements of transient loss is therefore vital to the understanding of the laser operation.

The marked decrease in absorption at 250 ns in the laser discharge could be accounted for by discharge constriction, which reduces the absorption path in the active volume to a small fraction of the original length. This observation by itself is not sufficient evidence for concluding that constriction is occurring. However, in the next two sections, we shall see that other phenomena, occurring in the discharge at the same times, point to the same cause, i.e., discharge constriction.

At the moment, no definite answer to the question of what causes the transient absorption can be given, nor can one species be ruled out (or included) in the contribution to absorption in a laser gas mixture on the basis of observations in partial mixtures (we carried out absorption measurements for various combinations of the gases which form the laser mixture, excluding one of them in turn, in order to single out particular absorption features of the various gas components).

A short list of likely candidates as species responsible for the transient absorption would include Cl^- (electron photodetachment), xenon atoms in an excited state (photoionization), XeCl* (photodissociation), and heavy ions and neutrals such as Xe_2^+, Ne_2^+, etc. Unfortunately, experimental values for the absorption cross sections of many of the above species, in particular heavy ions and neutrals in the UV range, are not known. There are, of course, many other species which could be present in the discharge. It is likely that no single species is responsible, but rather that the total absorption is made up of small contributions from many species. Clearly, the problem requires further investigation.

3. Time-resolved measurements of emission in the visible.

Figure 3 shows in block diagram form the apparatus which was used in the time-resolved studies of visible emission from the laser discharge. In all but a few cases the emission from the laser was viewed in « endlight » (i.e., along the 40 cm long optic axis). This was essential for observations at many wavelengths because of their comparatively low intensity of emission when viewed in « sidelight » (i.e., in direction perpendicular to both the electric field and the optic axis).

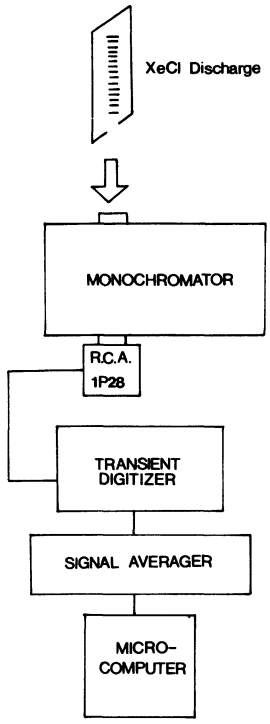

Fig. 3. — Experimental set-up for the acquisition of time-resolved discharge emission (see text for a full description).

In all the experiments the mirrors forming the laser cavity were removed and the Brewster angle windows were replaced by 3° off-axis silica windows. The unimpeded emission from the discharge was passed through a porthole in the screened room and imaged by a silica lens on the entrance slit of a 1m Cerny-Turner monochromator (Spex model 1802). The horizontal stripe image of the discharge formed on the entrance slit in such a way that (essentially) only the light emanating from the discharge region midway between the two electrodes of the laser was sampled. The monochromator was invariably used in 2nd order to maximise the spectral resolution. The monochromator could resolve 0.02 nm with both the entrance and the exit slit at minimum opening, and 0.04 nm with both slits open by a further 40 μm. In order to prevent higher order UV emission appearing when emission in the visible was being monitored, an appropriate filter was placed over the monochromator entrance slit (Corning glass n° 4784). The signal was detected at the exit slit by a photomultiplier (RCA, type 1P28) with specially modified circuitry for a fast signal risetime (~ 2 ns). A stepper-motor drive was attached to the monochromator to allow the wavelength setting to be increased by 0.01 nm steps reproducibly when a spectral feature was to be examined.

The signals from the photomultiplier were fed directly into a transient digitizer (Biomation model 8100), whose minimum temporal resolution was

~ 50 ns. Data from the digitizer were sent to a signal averager (Tracor Northern, NS-570 A) before subsequent transferral to a microcomputer (Research Machines 3802), and permanent storage on floppy disks. This was done for two reasons : firstly, the signal-to-noise quality of the signal could be monitored as the data for one particular wavelength point was collected (usually, the signal from 32 discharge events at one wavelength gave a good quality signal); secondly, the laser occasionally misfired and there was no method of detecting if the data was the result of a misfire unless it was monitored directly. A full spectral profile of an emission feature consisted of some 1000 data points.

Graphics software was used to produce the three-dimensional plots of intensity as a function of wavelength and time which are presented here. It was considered sufficient to monitor only the temporal evolution of a feature at line centre once one full spectral profile had been obtained.

Many xenon neutral and ion lines were monitored but, because all lines from a given species showed the same temporal behaviour, we present in this paper only the results for the XeI (excited neutral xenon) 467.123 nm ($7p[5/2]_3 \rightarrow 6s[3/2]_2$), and XeII (excited xenon ion) 484.433 nm ($6p\ ^4D^0_{7/2} \rightarrow 6s\ ^4P_{5/2}$) lines in emission, as representative results. We scanned a range of 3 Å, centred on line centre, for each line analysed.

The XeII 484.433 nm emission line is shown in the three dimensional plot of figure 4a (the normalized intensities of all the lines are expressed in arbitrary units). The intensity of this line was greater than any feature — other than XeCl* emission — in the range 300-600 nm. The XeI transient at 467.123 nm is shown in figure 4b. This line was also observed in « sidelight » and exhibited the same temporal behaviour.

A very significant and obvious feature is that emission from xenon neutrals was totally complementary to the ion emission : most intense in the initial stages of the discharge pulse and falling as the XeII emission rose. XeI emission in the « ringing pulses » was weak in both helium and neon buffered mixtures. The occurrence of strong emission from a high-lying ion energy level (the lower level of the 484.433 nm line is some 12 eV above the ion ground state) indicated that a dramatic change was taking place in the discharge at late times. We would like to stress at this point, that the time at which the ion emission increased is perfectly coincident with the time at which our photographs showed the discharge to constrict into a number of filamentary channels (see Ref. [2, 3]). Consequently, the behaviour of the emissions from the XeI and XeII transitions (as representative examples) were studied to identify their functional dependence on different discharge parameters.

Firstly, we studied the emission around 484 nm as a function of time and wavelength in a discharge which, except for the absence of HCl, was run under the

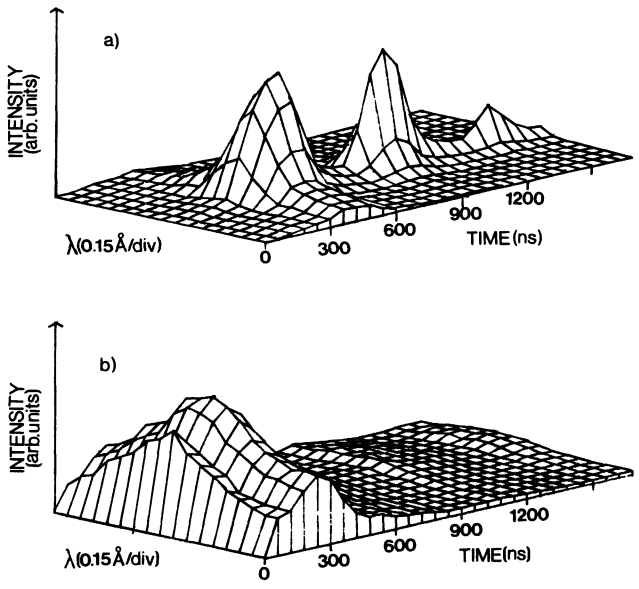

Fig. 4. — Time-resolved Xe ion (a) and neutral (b) emission spectra at 484.433 nm ($6p\ ^4D_{7/2} \rightarrow 6s\ ^4P_{5/2}$) and 467.123 nm ($7p[5/2]_3 \rightarrow 6s[3/2]_2$) respectively, from the same laser gas mixture of figure 2. It should be noted that in both plots the peak on the wavelength axis corresponds to the line centre, while the zero applies to time axis only.

same conditions as for a « normal » laser discharge. The important feature is that, in absence of HCl, the ion emission is barely detectable : emission in the region is dominated by the XeI-484.329 nm ($7p[3/2]_2 \rightarrow 6s[3/2]_1$) transition. In general, XeII emission initiates earlier as the HCl partial pressure increased; XeI emission, on the other hand, begins to terminate at precisely the time that XeII emission is increasing. The behaviour of XeCl* emission mirrors the XeI emission.

Secondly, we checked the effects on the XeI and XeII emission of variations of the buffer gas pressure. The buffer gas pressure shows to have only a little effect on the emission lines, in comparison to that caused by variation of the HCl partial pressure. Although there is a general trend of increasing XeI and XeII emission with Ne pressure, there appears to be a sharp transition in the nature of the discharge between 200 mbar and 600 mbar : XeI emission, from discharges with a total pressure of 600 mbar or more, terminates well before that observed at lower pressures.

Finally, the total discharge current effect on the XeI and XeII emission was monitored. There is a tendency towards earlier termination of XeI and earlier onset of XeII emission as the total discharge current is increased.

One further point to be made is that a brief scan of the entire emission spectrum between 300 and 600 nm indicated that xenon ion and neutral transitions were the only ones present: emission due to transitions in helium and neon was too weak to be

observed above the broad-band background emission.

A full discussion of the above results is postponed to section 5.

4. Time resolved measurements of absorption in the visible.

Temporally resolved absorption spectra were obtained using a similar method to that employed for transient absorption in the UV : trigger pulses from a « master » spark gap were sent *via* a variable length coaxial delay line to the respective « slave gaps » of the analyzed discharge and a short duration (15 ns) XeCl* laser (Oxford Lasers KX100) which provided the short UV pulse to optically pump a dye cell.

One type of dye — Coumarin 1 dissolved in methanol — was used exclusively since all the features of interest lay within its fluorescence spectrum (440-500 nm). Broad band fluorescence of the day was desiderable because, using the detection apparatus described below, an entire absorption profile could be obtained from a single discharge event. The intensity of dye emission was approximately two orders of magnitude greater than emission from the discharge under investigation in the spectral region of interest.

The fluorescence from the dye was directed through the XeCl* discharge using the same two slits employed in the UV transient absorption measurements.

As for the detection apparatus, the key piece of equipment was a microprocessor controlled optical multichannel analyser (« OMA »-Princeton Applied Research Corp., model n° 1215 processor, with a model n° 1254 SIT detector head incorporating a UV scintillator). The importance of this device lay in the speed at which an entire absorption spectrum could be recorded. It is important only to appreciate that this device made it possible to record, in a single discharge event, a 500 point intensity profile of both the probe and the reference signals as a function of wavelength.

The OMA detector head was mounted directly onto a monochromator (SPEX, model 1802) in the exit focal plane centered on the position normally occupied by the exit slit : the spectral region which could be scanned was determined by the dispersion of the monochromator at the wavelength of interest. Spectra were always recorded in the second order of the grating. The dispersion at a wavelength of 450 nm was such that a 5 nm wide spectrum could be recorded on a single shot. The resolution of individual spectral features was limited by the diode spacing of the OMA detector head to 0.025 nm.

Individual spectra from both the probe and the reference beams were collected simultaneously from one discharge event. The OMA microprocessor was used to automate the entire experiment. An « experiment start » pulse from the OMA switched a HV pulsar box which, subsequently, triggered the master spark gap. The processor commenced the scanning of the detector head 1 μs after receiving an « experiment stop » pulse from a photodetector.

In addition to automating the data collection process, the OMA microprocessor was used to perform all the data analysis. At each parametric data point, the spectral profiles of each of approximately twenty shots were collected. Each reference profile was divided by the corresponding probe profile before averaging.

Curves of the absorption coefficient K_λ were obtained by taking the natural logarithm of each (normalised) mean spectral intensity ratio and dividing by the 38 cm absorption path length. The value of $\int K_\lambda \, d\lambda$ for each parametric data point was obtained using an OMA integrating function which summed the magnitudes of K_λ over an operator-specified number of wavelength channels.

By using the measured values of K_λ we performed the following calculations :

1) The time resolved population of the $6s[3/2]_2$ XeI (metastable) level through absorption by the $6s[3/3]_2 \rightarrow 7p[5/2]_3$ (467.123 nm) transition in a normal laser gas mixture (see Fig. 5).

2) The time-resolved population of the $6s[3/2]_1$ XeI (resonance) level through absorption by the $6s[3/2]_1 \rightarrow 7p[5/2]_3$ (482.971 nm) transition in a normal laser gas mixture (Fig. 6).

3) The time-resolved population of the $6s\ ^4P_{5/2}$ XeII level through absorption by the $6s\ ^4P_{5/2} \rightarrow 6p\ ^4D_{7/2}$ (484.433 nm) transition in a normal laser gas mixture (Fig. 7).

In order to calculate the above populations we used the following expression (see Ref. [10], for example) :

$$N_i \simeq \frac{g_i}{g_j} \frac{9\pi c}{\lambda^4 A_{ji}} \int_{\text{line}} K_\lambda \, d\lambda \qquad (1)$$

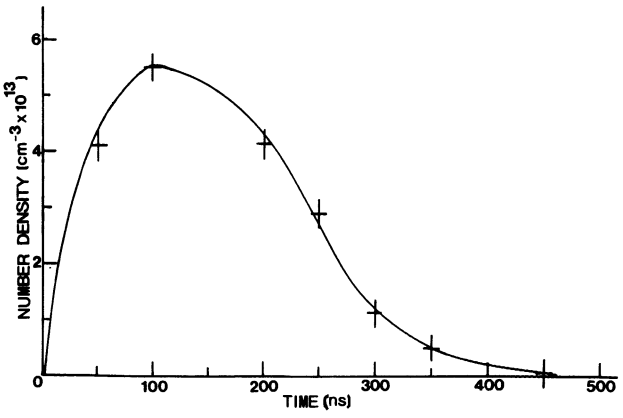

Fig. 5. — XeI-$6s[3/2]_2$ (metastable) population *versus* time. This measurement and the ones of figures 6 and 7, were performed in the same normal laser gas mixture of figures 2 and 4.

where N_i is the population in the energy level i from which absorption takes place, c is the speed of light. λ the wavelength, A_{ji} the spontaneous transition probability (from j to i level, ji) and g_i and g_j the statistical weights (degeneracy) of the levels. In equation (1) it is assumed that λ does not vary significantly over the absorption feature and that the upper level population is small. The values of A_{ji} used for the two XeI transitions are the most recently available experimental values [11].

The transition probability quoted for the XeII transition is merely the inverse of the upper level ($6p\ ^4D^0_{7/2}$) lifetime measured in reference [12]. Since its use contains the assumption that radiative decay occurs only to the 6s $P_{5/2}$ level, this value will represent an upper limit on A_{ji}, and, therefore, a lower limit on the calculated number density of the 6s $^4P_{5/2}$ level.

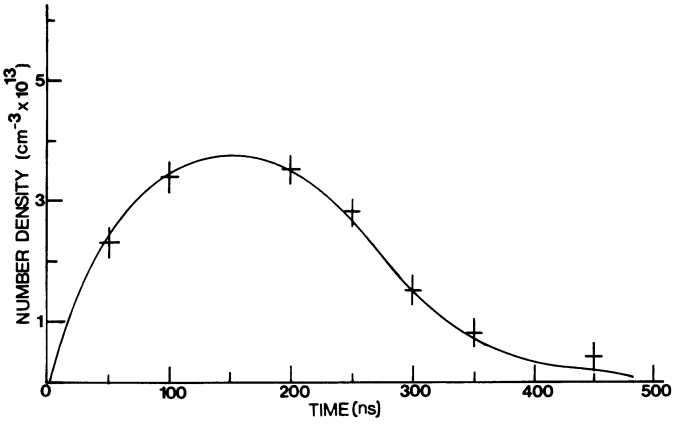

Fig. 6. — XeI-6s[3/2]$_1$ (resonance) population *versus* time.

It must be stressed that the number densities in figures 5-7, were calculated on the basis of a constant 38 cm absorption path length. Moreover, the error bars only provide an indication of the uncertainty in the measurement of $\int K_\lambda \, d\lambda$ from the absorption spectra, they do not include uncertainties in transition probabilities (A_{ji}).

As can be easily seen in figures 5-7, which refer to the same experimental conditions (gas mixtures, partial pressures, input energy, etc.) given in the introduction, the temporal evolution of both the XeI (metastable) and XeII populations show a marked similarity to the temporal evolution of the corresponding emission features presented in section 3. The XeI metastable population exhibits a sharp rise after discharge initiation but then begins to fall after 200 ns has elapsed. The behaviour of the population of the XeI resonance level with time is, within experimental errors, exactly the same. On the other hand,

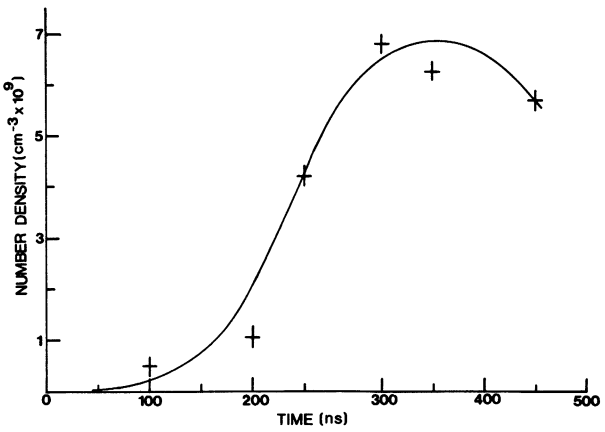

Fig. 7. — XeII-6s $^4P_{5/2}$ population *versus* time.

the XeII-6s $^4P_{5/2}$ number density *does not rise until late* in the 500 ns discharge pulse, and it remains high until pulse termination.

Finally, we note that large increases in the total discharge current (achieved by changing the number of cables in the pulseforming-network of our laser) have a comparatively small effect on the XeI metastable population. It would appear that the discharge is operating close to a point in which the population becomes independent of the electron density. Probably, limitation on XeI metastable population at high electron density values is due to 2nd order collisions and ionization from excited states.

5. Discussion of the experimental results and conclusions.

The presence of the XeII emission and its temporal connection with the discharge constriction is a key feature of our experimental results.

Excitation to the high-lying upper levels (26 and 28.5 eV above the xenon neutral ground state) of the observed ion transitions will be dominated by electron impact. Given this fact, it could be postulated that single-step ionization from the neutral ground state is responsible. However, this proposal can be rejected by the following-simple argument : under the same discharge conditions and at the same time, little, if *any*, emission is detectable from either neon or helium excited state transitions. This is despite the fact that the ground state density of the buffer gas is two orders of magnitude greater than the ground state xenon density, and that the energy required for excitation of He and Ne is less (1.5 eV in helium and 4.5 eV in neon) than that required for single-step excitation to the XeII-6p $^4D^0$ levels.

Thus, the only plausible process by which excitation might occur is multi-step excitation *via* the XeII ground state. In the case of multi-step excitation *via* the ion ground state, the population in the excited state will have *at the very least* a linear dependence

on the electron density. This arises because the ground state XeII density is dependent only on the electron density (charge neutrality), and can be easily seen by recalling the following equation for the rate process balance giving the ratio of the density of atoms in an upper state N_j (an XeII excited state in this case), to that in a lower state N_i (XeII ground state), assuming domination of excitation by electron impact :

$$\frac{N_j}{N_i} = \frac{n_e S_{ij}}{n_e d_{ji} + A_{ji}} \tag{2}$$

where n_e is the electron density, S_{ij} is the rate coefficient for excitation, d_{ji} the total electron collision destruction rate of level j, and A_{ji} is a coefficient representing losses by processes not involving electrons. Thus, even in the case of $n_e d_{ji} \gg A_{ji}$, where the n_e terms in both the numerator and denominator of equation (2) cancel, an n_e dependent term still remains.

The linear dependence on n_e represents the minimum case : that of one 13-14 eV step from the XeII ground state to the 6p ^{4}D levels. It is very likely that excitation will be influenced considerably, and perhaps dominated, by processes involving excitation of the ion in more than one step. For example, a simple calculation indicates that the rate for a two-step excitation process is 10 times greater than that of single step excitation from the ion ground state, solely on the basis of the difference in the threshold energy for the excitation.

The conclusion which is arrived at, then, is that the observed XeII emission is brought about by many step excitation of xenon neutral atoms *via* the ion ground state as a direct result of an increase in the electron density. The number density of the upper level of the 484.433 nm transition will be at the very least linearly dependent on the electron density, and possibly (assuming two steps from XeII ground state) have a cubic dependence on n_e.

In the above qualitative discussion, we assumed that the Xe^+ population is a constant fraction of the electron density. This simplifying assumption is based on the fact that the ion density follows the electron density, since the very small Debye length implies charge neutrality on a local basis ; moreover, Xenon has — but for HCl, which has, however, a density 10 times lower than Xe — the lowest ionization potential of the gas mixture (the buffer gas ionization potential is twice that of xenon, and, moreover, we observed no emission from excited Ne or He atoms).

The implications of a requirement for an increase in the electron density on the macroscopic parameters of the discharge becomes evident remembering that :

$$n_e = \frac{I}{eAv_d} \tag{3}$$

where I is the discharge current, e the electronic charge, A the cross-sectional area through which current flows, and v_d the electron drift velocity.

In the case of a normal gas mixture (2-3 mbar HCl), the change in the discharge voltage and current over the entire 500 ns is small 5 % at most. In particular the voltage shows a slight drop in the last 200 ns, while the current shows a corresponding slight increase. An increase in electron density at constant gas density can, therefore, only be accounted for by a *reduction* in the cross-sectional area for current flow A, i.e., discharge constriction.

The drop in the XeI excited state density is consistent with this conclusion. As was shown in the previous section the XeI excited state population is saturated with respect to the electron density ; thus, its number density will be a function of the electron temperature alone. The electron temperature would be expected to fall with the observed drop in discharge voltage and a consequent fall in the population would therefore be expected. However it must be noticed that the principal cause of the drop in number density indicated in figures 5 and 6 is the assumption of constant absorption path length. In fact, due to discharge constriction, the absorption path length is time-dependent, and this dependence is not included in the calculation. Obviously, the same consideration holds true for the XeII excited state population.

In conclusion, our experimental studies of emission and absorption in a long duration XeCl* laser discharge show a number of interesting features which can be related to our previous findings on discharge constriction (Ref. [1] and [2]). In particular, there is no XeII emission in absence of HCl and, as the partial pressure of HCl is increased, the time of onset of XeII emission moves steadily closer to the time of discharge initiation. Reduction in the XeCl* and XeI emission and voltage, and the increase in total discharge current, all occur at the same time that XeII emission is seen to increase. Furthermore, the time of onset of XeII emission is indicative of the onset of temporal volume constriction.

References

[1] HOGAN, D. C., BRUZZESE, R., KEARSLEY, A. J. and WEBB, C. E., *J. Phys. D* **14** (1981) L 157.

[2] HOGAN, D. C., KEARSLEY, A. J., WEBB, C. E. and BRUZZESE, R., in « Excimer Lasers 1983 » (Eds. C. K. Rhodes, H. Egger and H. Pummer), A.I.P. Conference Proceedings, **100** (A.I.P., New York 1983) p. 1-5 ;
BRUZZESE, R. and HOGAN, D. C., *Nuovo Cimento* **76B** (1983) 54.

[3] TAYLOR, R. S., private communication (1983).

[4] LEVATTER, J. I. and LIN SHAO-CHI ; *J. Appl. Phys.* **51** (1980) 210.

[5] LEVATTER, J. I. and LIN SHAO-CHI, *J. Appl. Phys.* **52** (1981) 1651.

[6] DOUGLAS, D. H. and MANI, S. A., *J. Appl. Phys.* **45** (1974) 4406.

[7] EDGLEY, P. D. and VON ENGEL, A., *Proc. R. Soc. London* **A 370** (1980) 375.

[8] EMELEUS, K. G. and WOLSEY, G. A., *Discharge in Electro-negative Gases* (Taylor and Francis London) 1980.

[9] NABATA, K. and KANDA, M., *J. Appl. Phys.* **50** (1979) 3956.

[10] THORNE, A. P., *Spectrophysics* (Chapman and Hall and Science Paperbacks, London) 1974.

[11] RICHOU, J., *J. Quant. Spect. Radiat. Transfer* **23** (1980) 473.

[12] MOHAMED, W. A. and KING, G. C., *J. Phys. B* **12** (1979) 2809.